UCRL-JC--104372

DE91 004881

Simulations of NOVA Direct-Drive Rayleigh-Taylor Experiments*

APS Division of Plasma Physics, Cincinnatti, November 12-16, 1990

S. V. WEBER
Lawrence Livermore National Laboratory
P.O. Box 808
Livermore, CA 94550

Directly driven Rayleigh-Taylor instability growth experiments being performed on NOVA have been simulated using the computer code, LASNEX. These experiments employ beams smoothed with random phase plates (RPP), and will later include smoothing by spectral dispersion (SSD). Samples are CH foils with or without imposed sinusoidal surface perturbations. Perturbation growth is diagnosed by means of x-ray backlighting. Calculated growth rates are fairly flat across the wavelength range of 20 - 80 μm which can be accessed experimentally, and are moderately suppressed below classical growth rates. Perturbations of large enough initial amplitude that the contrast in the x-ray image is measurable from the start of the experiment quickly grow into the nonlinear regime. Smaller initial amplitudes result in a longer interval of linear growth, but the initial perturbation will not be detectable in the data. Structure which is predicted to develop from speckles in the RPP beam pattern, with and without SSD, is also presented.

The direct-drive Rayleigh-Taylor experiments to be conducted on the NOVA laser have two principle objectives. The first is to test the beam smoothing implementation. Direct drive requires a beam which is smooth enough that a sample can be pushed for a distance equal to many (perhaps 10-30) times its initial thickness. Single wavelength Rayleigh-Taylor experiments require a beam which is uniform enough that perturbations due to beam nonuniformities do not overwhelm those due to the imposed surface perturbation. NOVA beam smoothing will employ random phase plates (RPP), smoothing by spectral dispersion (SSD), and optical wedges. RPP and SSD were invented at the Laboratory for Laser Energetics at the University of Rochester[1]. The NOVA implementation of these techniques differs in some respects from that employed by LLE. LLE will collaborate with LLNL for these experiments.

The second objective of these experiments is to test modeling of Rayleigh-Taylor perturbation growth. Modeling predicts that growth rates will be reduced below the classical value by density gradient and ablative stabilization. We will look at the growth of perturbations beginning from a single wavelength, to see the growth rate and nonlinear coupling to harmonics of the initial mode. Later experiments may begin with multiple-wavelength initial surface perturbations. The experiment objectives are summarized in figure 1.

Gail Glendinning is the principal experimentalist for this series. Mark Henesian is in charge of the implementation of SSD. The laser science is under the

*This work was performed under the auspices of the U.S. Department of Energy by Lawrence Livermore National Laboratory under contract No. W-7405-Eng-48.

* This work supported by DoE contract No. W-7405-ENG-48.

DISTRIBUTION OF THIS DOCUMENT IS UNLIMITED

MASTER

direction of Howard Powell. Sham Dixit has provided modeling of the laser spot intensity distribution, while the author has modeled the target physics.

The beam smoothing on NOVA will be implemented on one beam on the two-beam chamber, because of easier access to the beam and the presence of extensive beam diagnostics. The beam will be frequency-doubled to 0.53 μm. The beam smoothing implementation employs three elements, listed in figure 2. Random phase plates are an array across the beam aperture of small phase plates which introduce delays of either zero or one-half wavelength. These break up the beam coherence, and produce a far-field spot pattern with an Airy disk envelop, with a diameter corresponding to the diffraction limit of a single phase plate element. This envelop is modulated by small scale speckle, with a size determined by the diffraction limit of the entire aperture. For NOVA, the Airy disk diameter resulting from 3.5 mm phase elements is about 1100 μm, while the individual speckle size is about 7 μm.

The small scale speckle from RPP on a coherent laser beam is fixed in time, and we predict that such a beam does not give sufficiently uniform illumination. In SSD, bandwidth is introduced into the laser, and different frequencies are separated spatially by means of a grating. Interference between the different frequencies at focus causes the speckle pattern structure to change rapidly, so that the average over hydrodynamic timescales important to the target is fairly smooth. On NOVA, bandwidth will be introduced by cross-phase modulation. The drive pulse is co-propagated through a fiber with a modulating beam of perpendicular polarization. We will explore two schemes of modulation. Periodic or sinusoidal phase modulation uses a coherent modulating beam, which we will tune to produce a modulation frequency of 45 Ghz. This will give a speckle pattern which repeats periodically every 22 ps. Noisy phase modulation will use a modulating beam from a noisy oscillator, so that the speckle pattern does not repeat. In both cases, the laser bandwidth will be about 15 Å in 1 μm light, and 7.5 Å in green light. The noisy phase-modulated beam has been propagated though NOVA without separating colors with a grating. Propagation of the SSD beams with the two modulation schemes will have to be explored to test damage limits resulting from significant beam intensity fluctuations.

As RPP's give a centrally-humped spot profile, we have employed optical wedges to separate segments of the beam into a roughly square pattern. The wedges are in a 3 x 3 array aligned with the frequency conversion crystal egg crate. The wedges give a spot with a flat intensity central section of about 600 x 600 μm within which the intensity (neglecting speckles) is uniform to within about 10%. Figure 3 shows an image of the actual NOVA spot with RPP and wedges. The speckle pattern modulation is apparent. The somewhat trapezoidal spot envelop results from use of a crystal array differing from that for which the wedges were designed. We anticipate a more uniform spot with the proper crystal array in later experiments.

The experimental setup is shown in figure 4, and described in figure 5. The single smoothed beam is used to drive the target foil. The opposing beam illuminates a backlighter. The backlighter is viewed through the foil by a gated x-ray pinhole camera (GPHC). The pinhole camera will give up to 18 frames with about 10 μm resolution, and a gate length of about 100 ps. A uranium backlighter

filtered with 25 μm of beryllium will give a backlighting spectrum peaked around 1.5 keV. Backlit images will show modulation in column density through the target. Some shots will employ embedded seeded layers in the target. A streaked spectrometer will be used to look for line emission from the seed. Nonuniform ablation of the foil will be indicated by earlier-than-expected emission from the seeded layer as in the experiments of Delletrez et al.[2] Another GPHC will attempt to resolve spatially the line emission from the seeded layer. We may use bromine for the seed, which will give L-lines. An alternative would be chlorine, which would give K-lines, which might be easier to interpret, but would require a higher temperature to excite. Foil acceleration will be measured in shots which are backlit from the side, and viewed with a streaked pinhole camera (SPHC).

Sample properties are listed in figure 6. Typical samples will be CH foils about 20 μm thick. An opaque carbon overcoat will suppress early shine-through of the laser light, which has been seen in LLE experiments. Carbon is used to avoid interference with the bromine seed lines. The laser intensity profile to be used is a linear ramp lasting 1 ns, followed by a 2 ns flat-top to give fairly constant foil acceleration. Depending on the beam energy which we can achieve, the peak laser intensity will be 0.7 - 1.5 x 10^{14} w/cm^2. For samples with imposed surface perturbations, the wavelengths will be in the range 20 - 100 μm, and amplitudes 0.2 - 3 μm peak-to-valley. The maximum calculated Rayleigh-Taylor growth is at shorter wavelengths, of order 10 μm, which is expected to be beyond our resolution limit. The smaller initial amplitudes will not give measurable initial contrast in the backlit image, but permit more growth before saturation. Also, as we shall see later, the lower initial amplitudes require a very smooth laser beam.

An outline of the experimental campaign is shown in figure 7. SSD hardware is not yet in place on NOVA, so experiments in November-December, 1990, will employ RPP and optical wedges alone. These experiments will employ foils without imposed surface perturbations, as we predict that the beam will not be smooth enough to accelerate intact foils very far. We expect to see early breakup of the foils and to measure ablation rates 50-100% greater that those predicted by 1-D calculations. These initial experiments are intended for diagnostic checkout, and for comparison with later experiments with SSD.

We expect to have SSD in place on NOVA by early 1991. The first SSD shots will also use flat foils. We hope that some implementation of SSD will give sufficiently uniform acceleration of the foils that we can continue to experiments with surface perturbations. These will probably not begin until spring, 1991. In this presentation, we do not discuss the analysis of experiments with surface perturbations in much detail, but the methods will be similar to those of the indirect drive experiments, which are presented by Remington et al., in poster 3E7 at this meeting.

Modeling of the targets uses the LASNEX computer code. Hydrodynamics is fully lagrangian. Laser energy is deposited by a large number (typically ~1000) of traced rays. The ray angles are varied randomly every cycle to minimize variations in laser intensity resulting from ray statistics. Speckle calculations impose power variations upon the rays so as to yield the desired intensity pattern at the focal plane, in the absence of refraction. Without wave optics in the code, it is not possible to reproduce the depth dependence of the intensity pattern.

Electron conduction employs diffusion with a flux limit of 0.1. The speckle calculations use a new implementation of finite element conduction, which gives much smoother temperatures in distorted meshes than the regular finite difference scheme. Radiation from the corona is an important preheat source for the unablated portion of the foil. Some calculations employ multigroup radiation diffusion, while others input energy deposition from a 1-D calculation in order to reduce computation time. Bromine line intensities are calculated from non-LTE opacities generated by a statistical configuration accounting (SCA) package.

A central issue for these experiments is how uniform the laser intensity needs to be for laser intensity nonuniformities not to dominate surface perturbations. Figure 8 shows the Rayleigh-Taylor growth rate spectrum predicted from the formula of Takabe et al.[3] Although we model our experiments with explicit 2-D simulations to account for time dependence, finite amplitude, and other effects not included in the Takabe formula, qualitative feature of the growth rate spectrum agree well with this formula. Peak growth rate are predicted to arise at wavelengths of 5 - 20 μm, where the laser speckle spectrum has substantial power. SSD does not give completely smooth illumination. Figure 9 shows 50 μm-long slices through several intensity patterns. Curve **a** is an instantaneous speckle pattern, similar to the stationary pattern produced by RPP without SSD. The modulation rms/mean is a few. Curve **b** shows the time-average pattern from periodic SSD, which is reached after an averaging time of 22 ps. Modulation of about 20% rms remains. Curve **c** shows the average over 100 ps of the pattern calculated for noisy phase modulation SSD, which has a substantially better rms/mean ~ 8%. The first 25 μm of curves **a** and **b** are used for the 2-D RPP and SSD simulations described below. We have not yet calculated target acceleration with noisy SSD.

Figure 10 shows the growth in column density (ρr) fluctuations calculated for a single 40 μm wavelength mode, for a flat sample drive with stationary RPP speckle, and for a flat sample drive with periodic SSD. The speckle pattern imprints itself on the sample during the first roughly 500 ps before the critical surface stand-off becomes greater that the dominant wavelengths. After that, the perturbations grow by ablation front Rayleigh-Taylor instability. The modulation from the RPP speckle is comparable to that from the relatively large 2 μm initial amplitude surface perturbation. This large amplitude surface perturbation grows by about two e-foldings during the uniform acceleration interval after 1 ns, before becoming substantially nonlinear.The periodic SSD calculation is less modulated than that for RPP alone by about a factor of two. Clearly, a significantly smoother beam would be needed to see the growth of modulations with initial amplitudes a factor of ten smaller.

Figures 11a-c show density contours of the single wavelength calculation at a series of times. The laser is incident from the right. Due to symmetry, only half of a wavelength is modeled. All pictures employ equal horizontal and vertical scales. Figures 12a-c and 13a-c show the RPP and SSD calculations at the same times. The RPP calculation at 2 ns is getting punched through at the bottom edge, and the contour plotter has encountered difficulty with it.

Figure 14 shows the ablation depth as a function of time for uniform illumination (1-D), RPP, and periodic SSD. Curves **b** are spatially averaged,

whereas curves c show the maximum ablation depth across the simulated strip. During the steady acceleration interval after 1 ns, the maximum depth ablation rate is about twice the 1-D rate. Interestingly, the RPP and SSD ablation rates are quite similar, although the ablation front modulation is greater for RPP. Figure 15 shows the simulated intensity in the bromine lines for the 1-D and RPP simulations, for foils in which a 3% (by number) brominated layer is buried under 4 μm of pure CH. The line intensity comes up about 0.5 ns sooner in the RPP calculation, reflecting the maximum depth ablation rate. The early time intensities represent continuum, which has not been subtracted out.

These simulations indicate that in the experiments with RPP alone, which will begin this month, we should expect to see early foil breakup and early seed emission, indicating an enhanced ablation rate. Experiments early next year with periodic phase modulated SSD may also show too much foil modulation growth for us to attempt experiments with imposed surface perturbations. It is possible that the calculations are too pessimistic or that aberrations in the laser will produce additional smoothing of the time-average speckle pattern. We have not yet modeled foils driven with noisy SSD, but we expect two to three times less foil modulation that for periodic SSD, which should be good enough to drive foils with large initial surface perturbations. Such experiments may begin as early as spring, 1991.

REFERENCES

1. S. Skupsky, R. W. Short, T. Kessler, R. S. Craxton, S. Letzring. and J. M. Soures, "Improved laser-beam uniformity using the angular dispersion of frequency-modulated light", *J. Appl. Phys.*, **66**, 3456 (1989).

2. J. Delletrez, R. Epstein, M.C. Richardson, P.A. Jaanimagi, and B. L. Henke, "Effect of laser illumination nonuniformity on the analysis of time-resolved x-ray measuements in uv spherical transport experiments", *Phys. Rev. A*, **36**, 3926 (1987); J. Delletrez, D. K. Bradley, P. A. Jaanimagi, and C. P. Verdon, "Effect of Barrier Layers in Burn-Through Experiments with 351-nm Laser Illumination", LLE Report No. 208 (1990).

3. H. Takabe, L. Montierth, and R. L. Morse, *Phys. Fluids*, **26**, 2299 (1983).

objectives of NOVA direct-drive Rayleigh-Taylor experiments

test beam smoothing techniques

- require beam nonuniformities not to overwhelm effect of foil surface perturbations
- NOVA beam smoothing incorporates random phase plates (RPP), smoothing by spectral dispersion (SSD), and optical wedges

test modeling of Rayleigh-Taylor growth

- single and multiple - wavelength initial surface perturbations
- look for predicted ablative stabilization
- examine nonlinear coupling to harmonics of initial modes

experiments will be done in collaboration with University of Rochester

Figure 1.

Reference UCRL-JC-104372

NOVA beam smoothing techniques

random phase plate (RPP)

- produces smooth Airy disk spot envelop
- leaves fine scale (~7 μm) high modulation speckle

smoothing by spectral dispersion (SSD)

- interference of different frequencies causes speckle pattern to change very rapidly
- periodic phase modulation of laser leaves significant (~20% rms/mean) residual time-average speckle
- noisy phase modulation gives reduced small scale structure in long time average

optical wedges

- steer sectors of single drive beam into square pattern
- flat intensity spot center ~600 x 600 μm within 10% of peak intensity

Figure 2.

Reference UCRL-JC-104372

Wedges Are Used To Produce Large Flat-topped Spot

Wedges + Phase plates

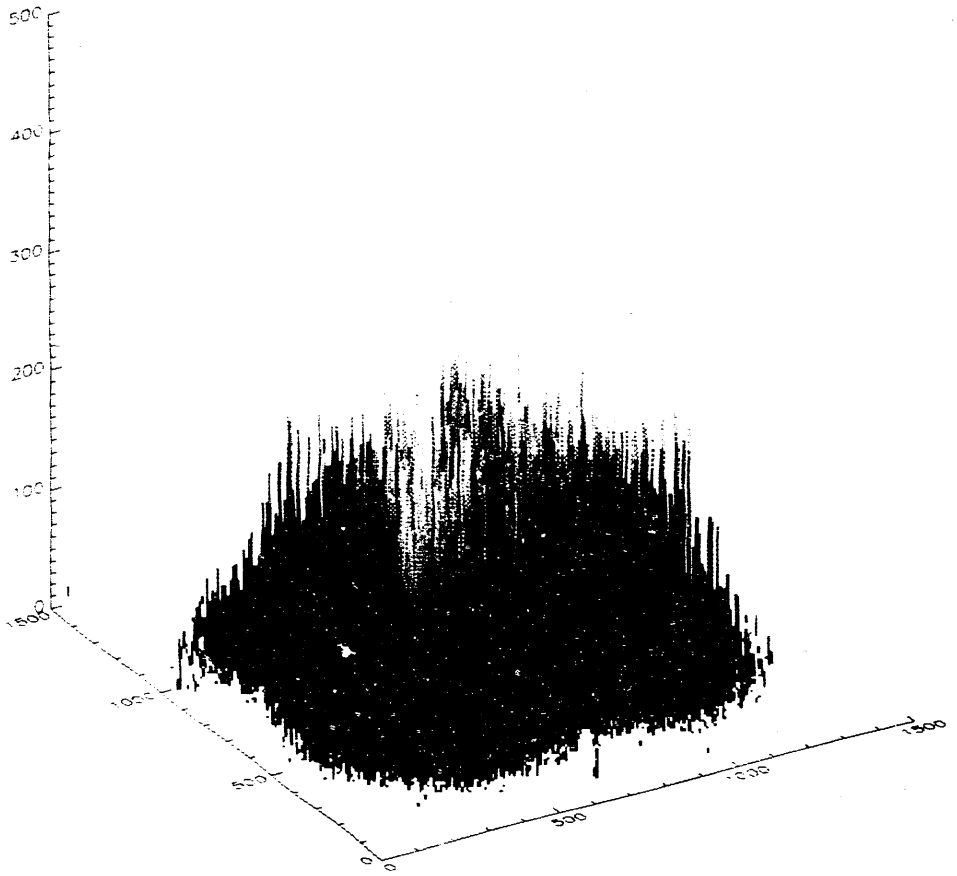

2300 µm

sgg_11190_1

Reference UCRL-JC-104372

Experimental Setup - Face On

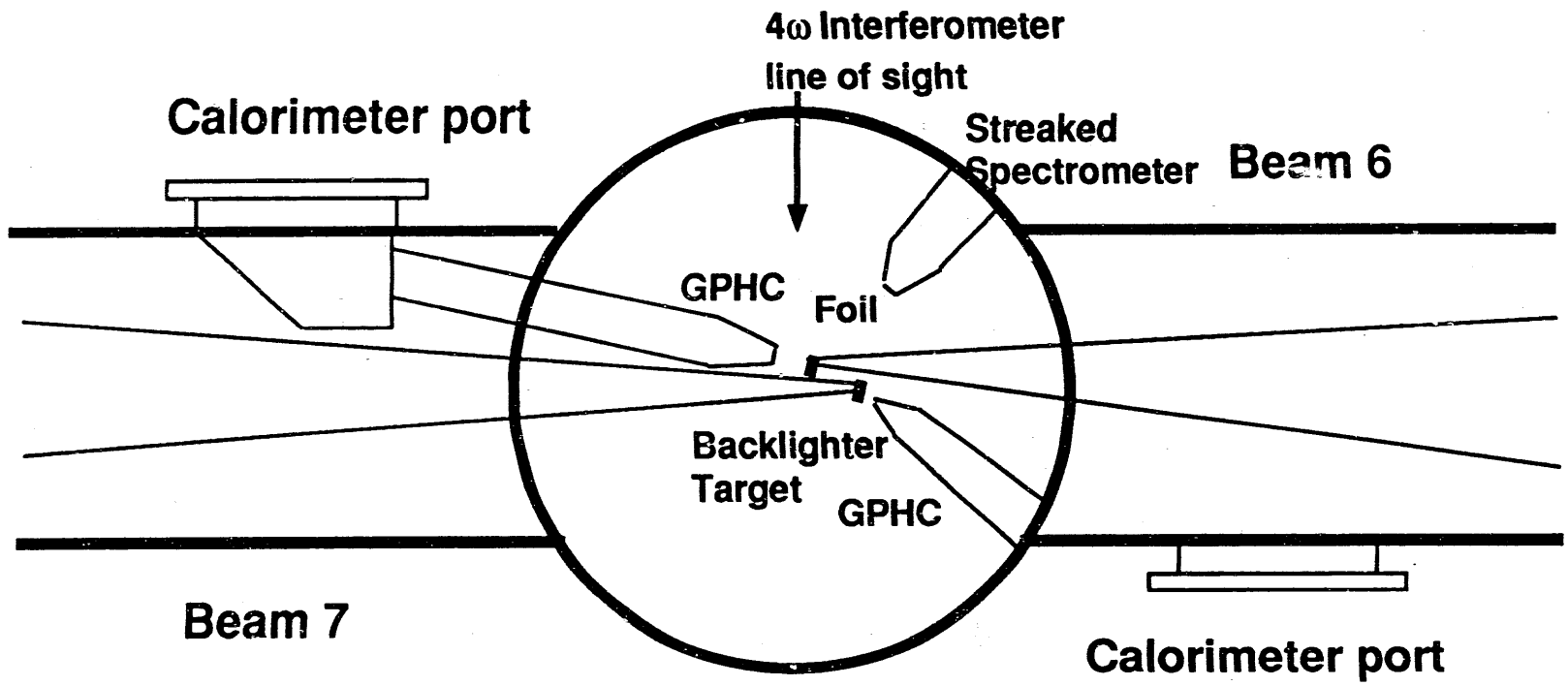

Top View

sgg-14890-06
Reference UCRL-JC-104372

principal diagnostics

gated x-ray pinhole camera

- face-on images with uranium backlighter show ρr modulation of foil
- 10 μm resolution, 100 ps gate, 18 images per shot

streaked spectrometer

- timing of line emission from embedded signature layer diagnoses ablation rate (following Rochester experiments of Delletrez et al.)
- may use chlorine K or bromine L line emission from seeded CH

another GPHC will attempt to spatially resolve line emission

streaked pinhole camera on side-lit shots will measure foil acceleration

Reference UCRL-JC-104372

Figure 5.

nominal sample properties

CH foil thickness ~20 μm

carbon overcoat (~0.1 μm) to prevent shine-through

imposed wavelength 20 - 100 μm

perturbation peak-to-valley 0.2 - 3 μm

peak laser intensity 0.7 - 1.5 x 10^{14} w/cm^2, 0.53 μm light

pulse profile 1 ns linear ramp followed by 2 ns flat-top

~2 - 4 kJ 2ω

Reference UCRL-JC-104372

Figure 6.

outline of experimental campaign

initial experiments will not have SSD (November-December, 1990)

- will employ foils without imposed surface perturbation
- we expect to see early foil breakup
- anticipate ablation rates 50-100% greater than 1-D calculation

SSD experiments will begin in early 1991

- propagation of beam through laser could be an issue
- will try both sinusoidal and noisy phase modulation
- hope some implementation will show adequate foil stability and 1-D ablation rate

experiments with single-wavelength surface perturbations will follow

- may begin in spring, 1991
- will proceed similarly to indirect drive experiments (see poster 3E7 by Remington et al.)

Figure 7.

Reference UCRL-JC-104372

Takabe formula predicts growth rates fairly flat with wavelength

$$\gamma = 0.9\sqrt{gk} - 3v_a k$$

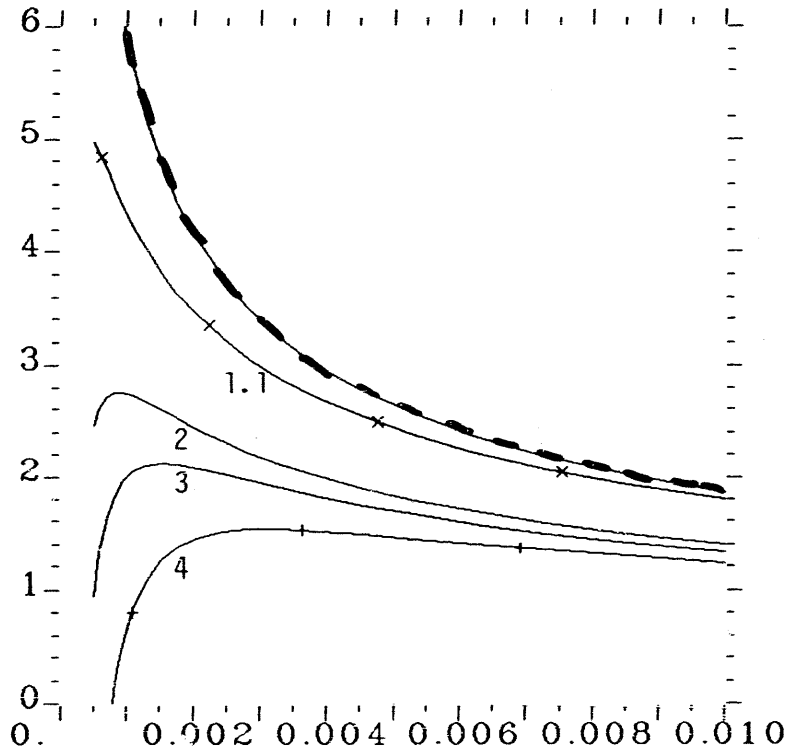

Takabe growth rate (/ns) vs. wavlength
at 1.1, 2, 3, 4 ns
dashed – classical for avg. accel.

Reference UCRL-JC-104372

Figure 8.

SSD leaves significant intensity modulation even in time-average

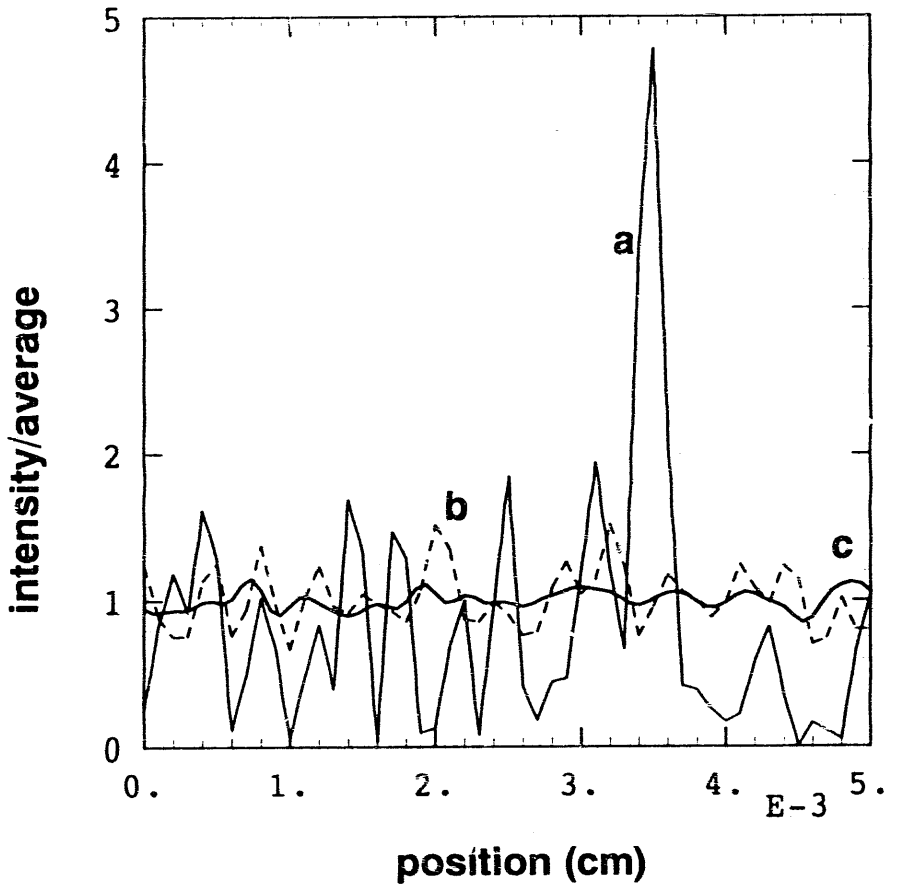

a - cut through instantaneous speckle intensity vs. position

b (dash) - time-average for 45 Ghz periodic phase modulated SSD (reached in 22 ps)

c (heavy solid) - average over 100 ps of noisy phase modulation SSD

Figure 9.

Reference UCRL-JC-104372

modulation driven by speckle is comparable to that from 2 μm surface perturbation

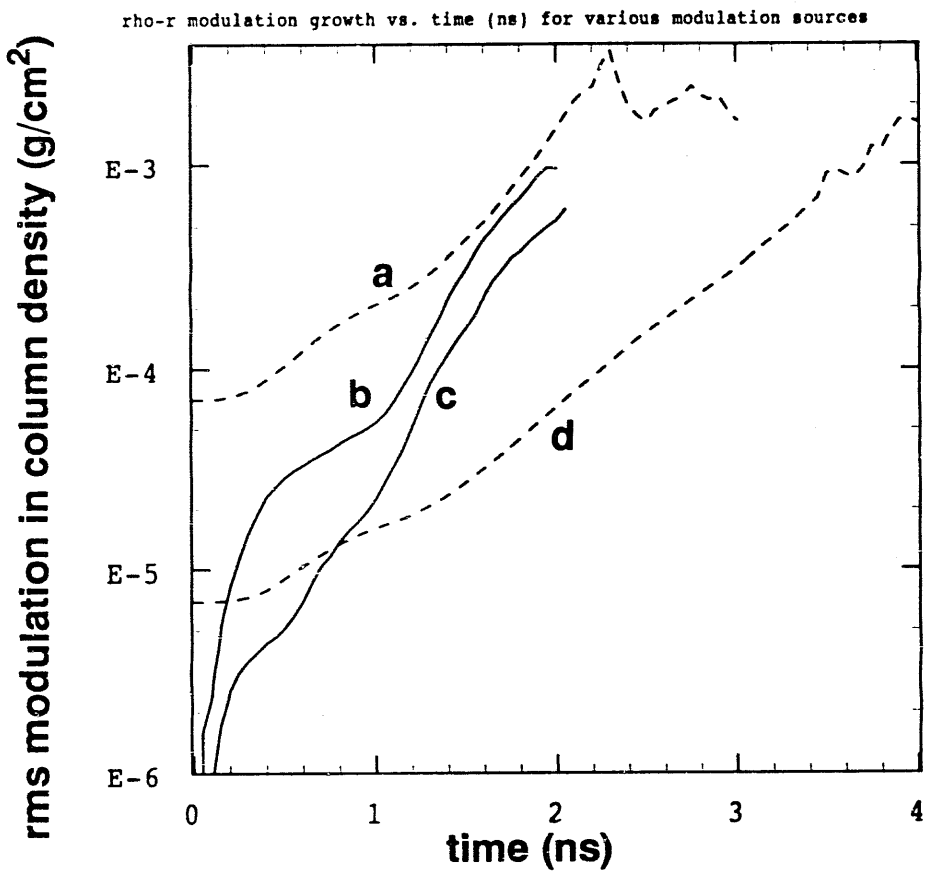

a - single 40 μm wavelength, 2 μm peak-to-valley
b - calculation driven with fixed RPP speckle pattern
c - calculation driven with time-dependent speckle pattern from periodic SSD
d - single 50 μm wavelength, 0.2 μm peak-to-valley

Figure 10.
Reference UCRL-JC-104372

growth of 40 μm wavelength initial 2 μm peak-to valley surface perturbation

simulation represents half of one wavelength

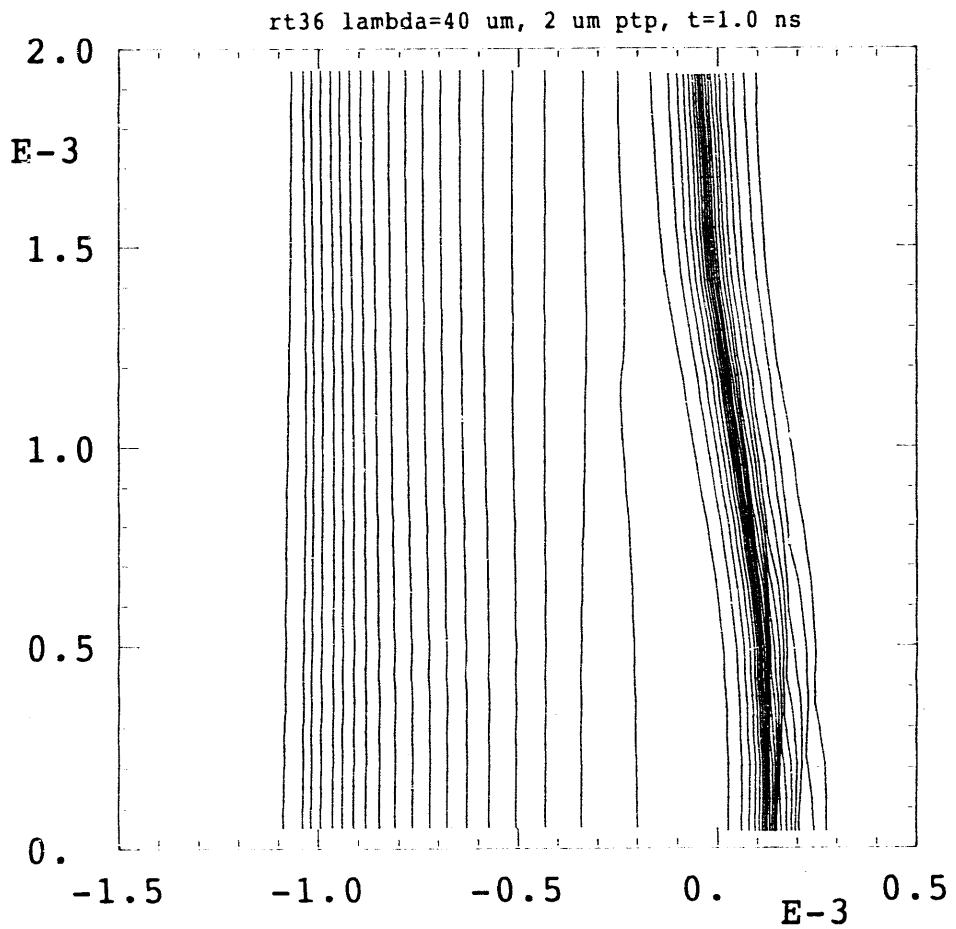

dimensions in cm

density contours

time = 1.0 ns

laser incident from right

initial left surface of foil at x = 0

Reference UCRL-JC-104372

Figure 11a.

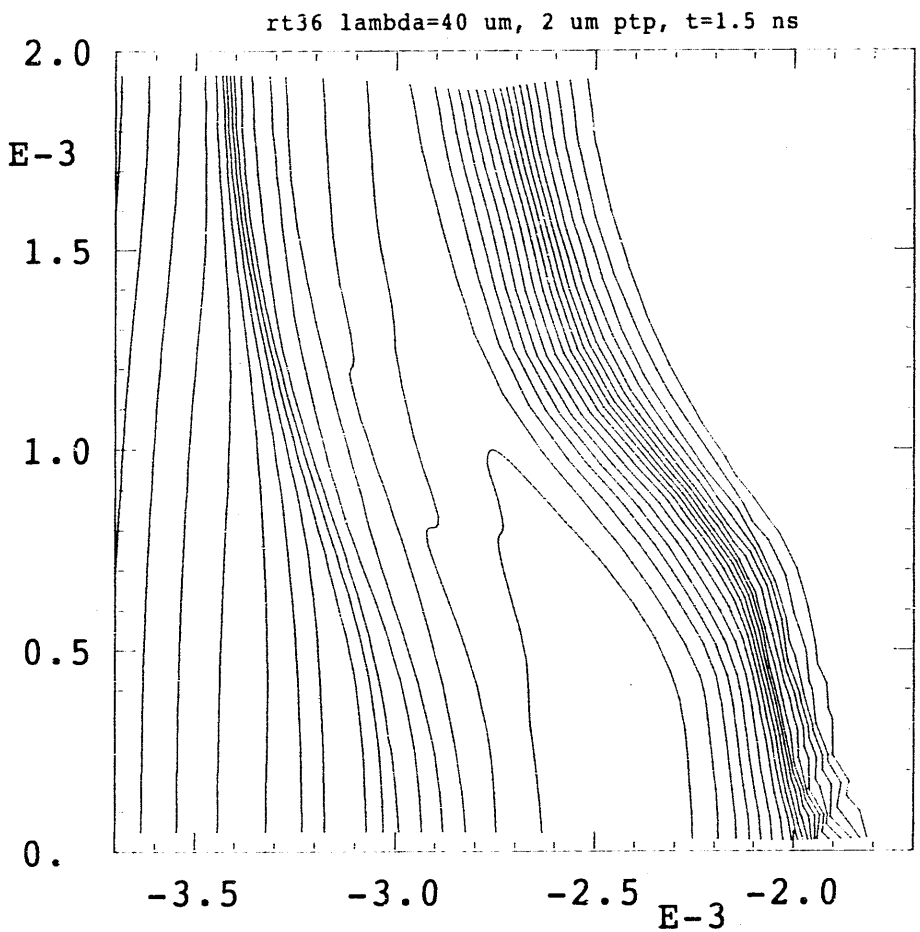

density contours

time = 1.5 ns

Reference UCRL-JC-104372

Figure 11b

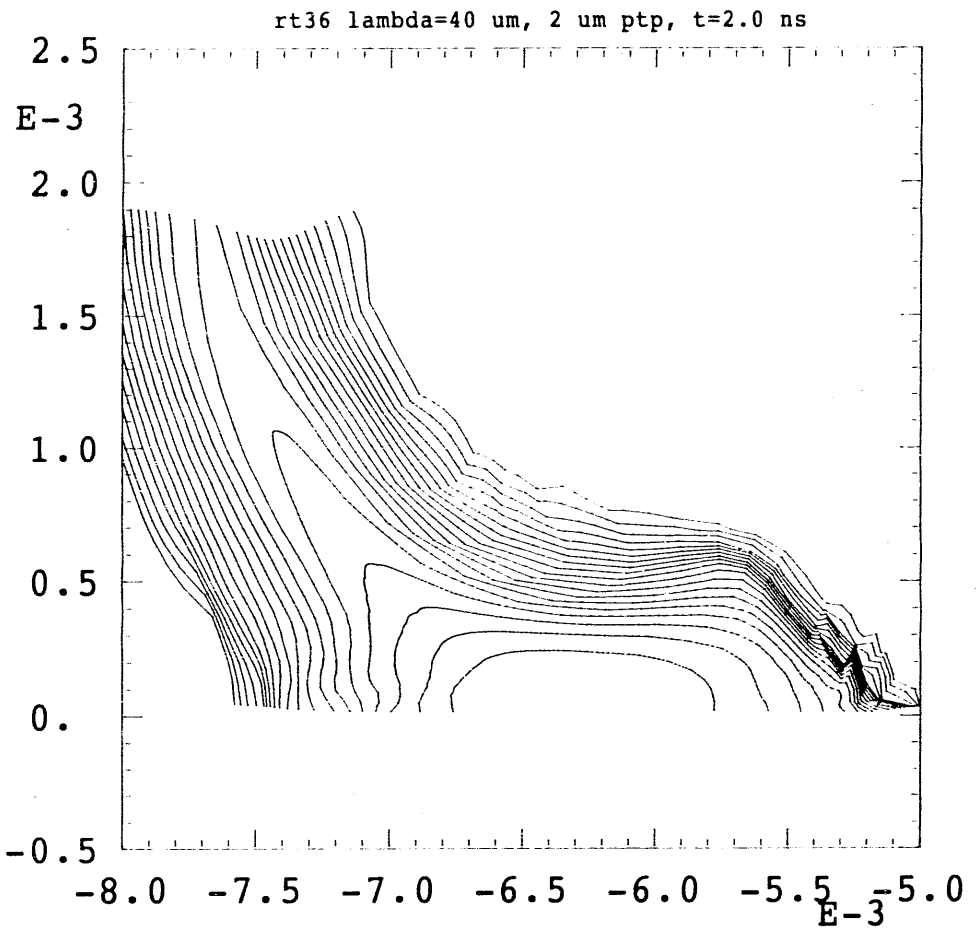

density contours

time = 2.0 ns

note scale change

Reference UCRL-JC-104372

Figure 11c.

growth of perturbations on flat foil from RPP stationary speckle pattern

2-D simulation of 25 μm slice

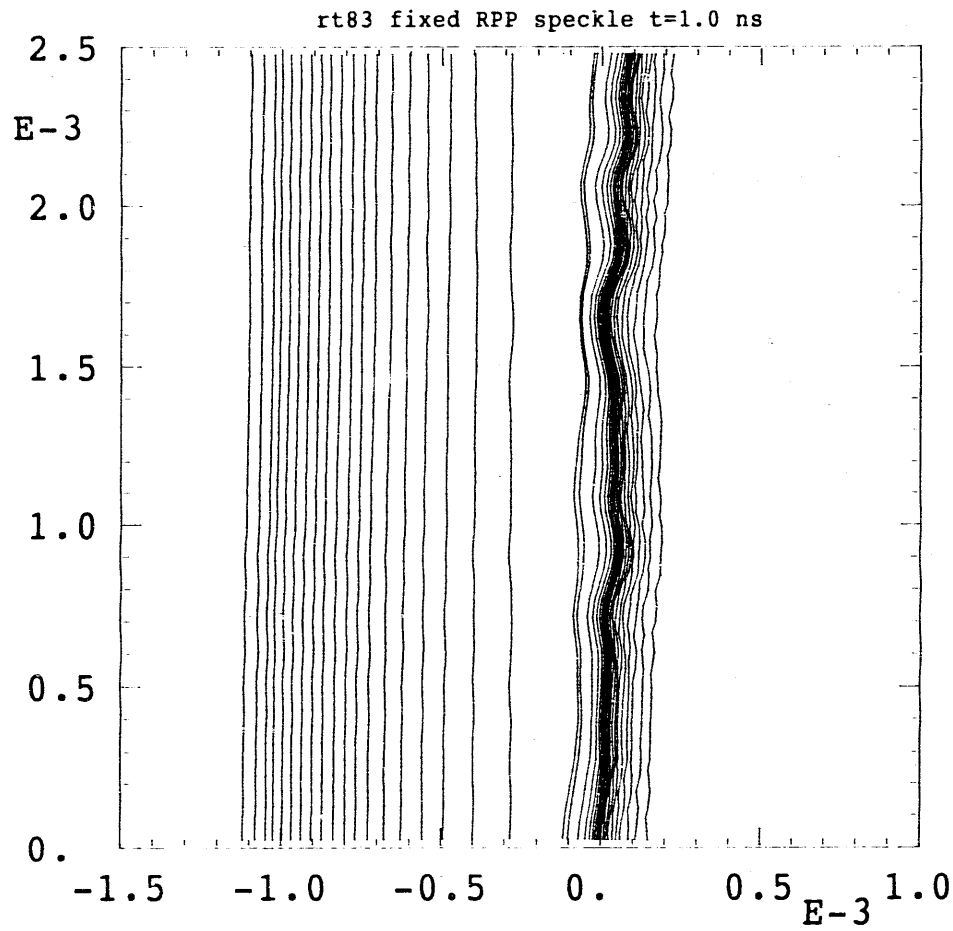

density contours

time = 1.0 ns

dimensions in cm

Reference UCRL-JC-104372

Figure 12a.

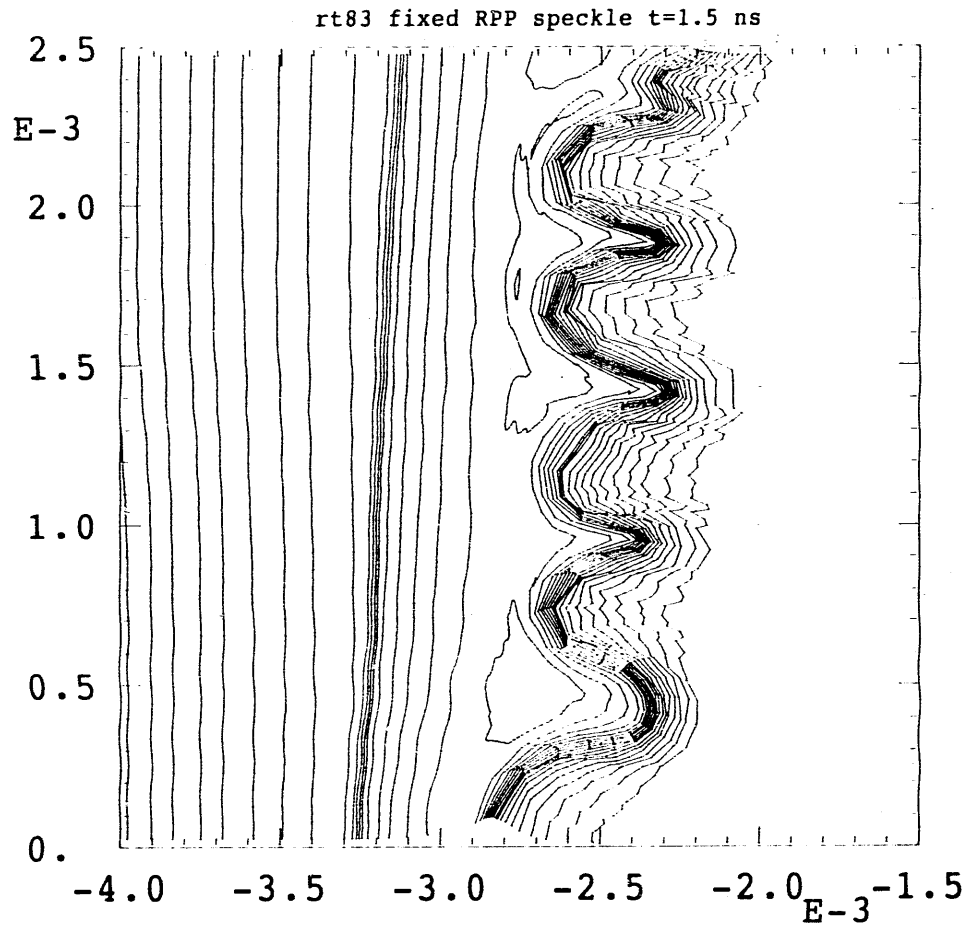

density contours

time = 1.5 ns

Reference UCRL-JC-104372

Figure 12b.

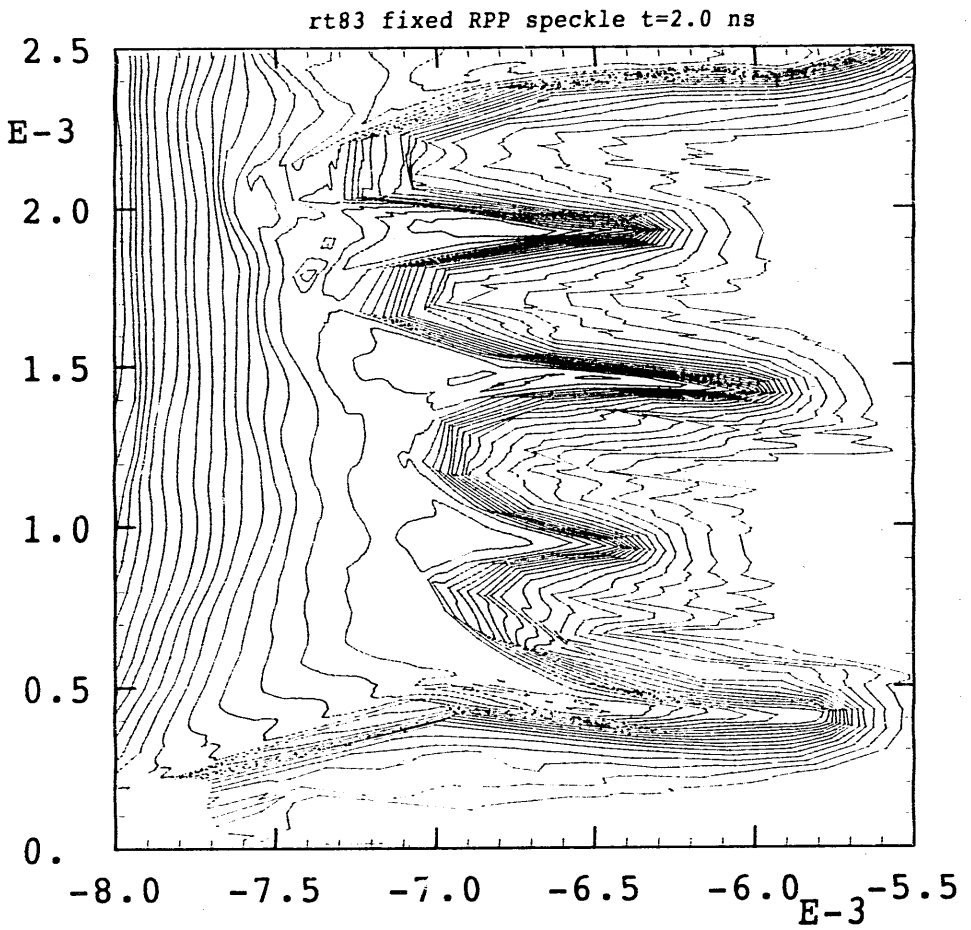

density contours

time = 2.0 ns

Figure 12c.

Reference UCRL-JC-104372

growth of perturbations on flat foil from SSD (45 Ghz periodic phase modulation)

2-D simulation of 25 μm slice

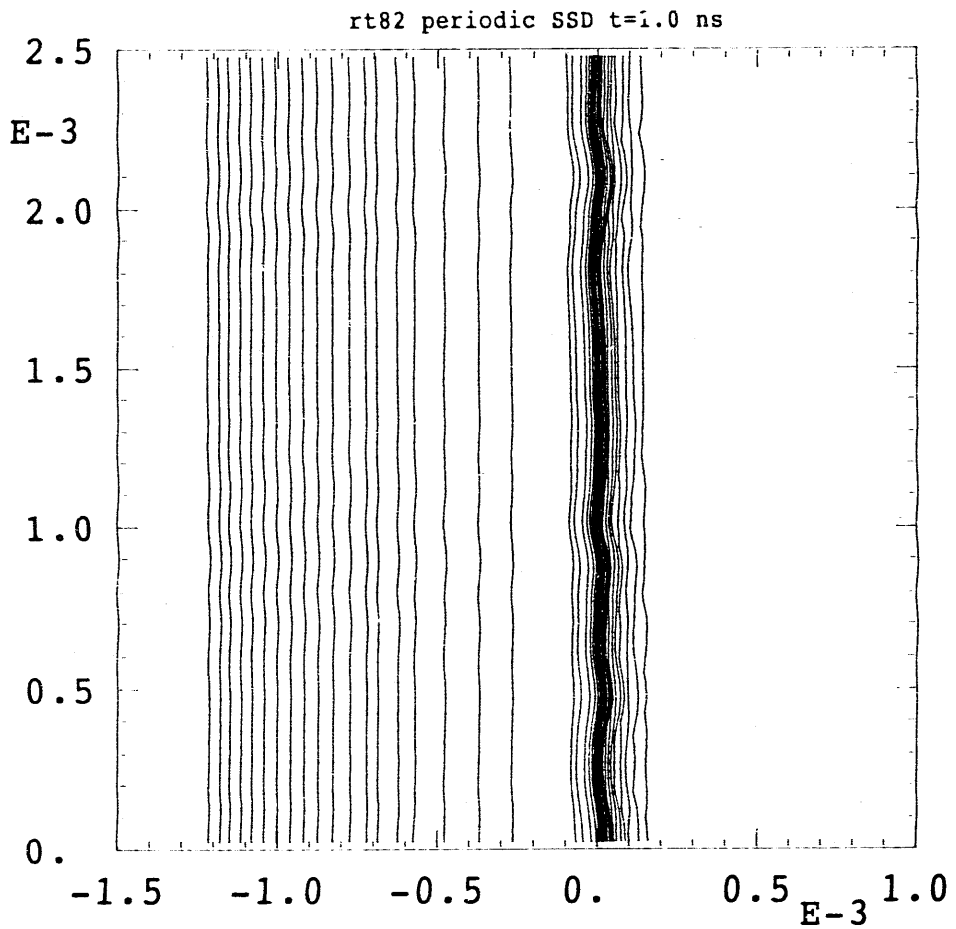

density contours

time = 1.0 ns

dimensions in cm

Reference UCRL-JC-104372

Figure 13a.

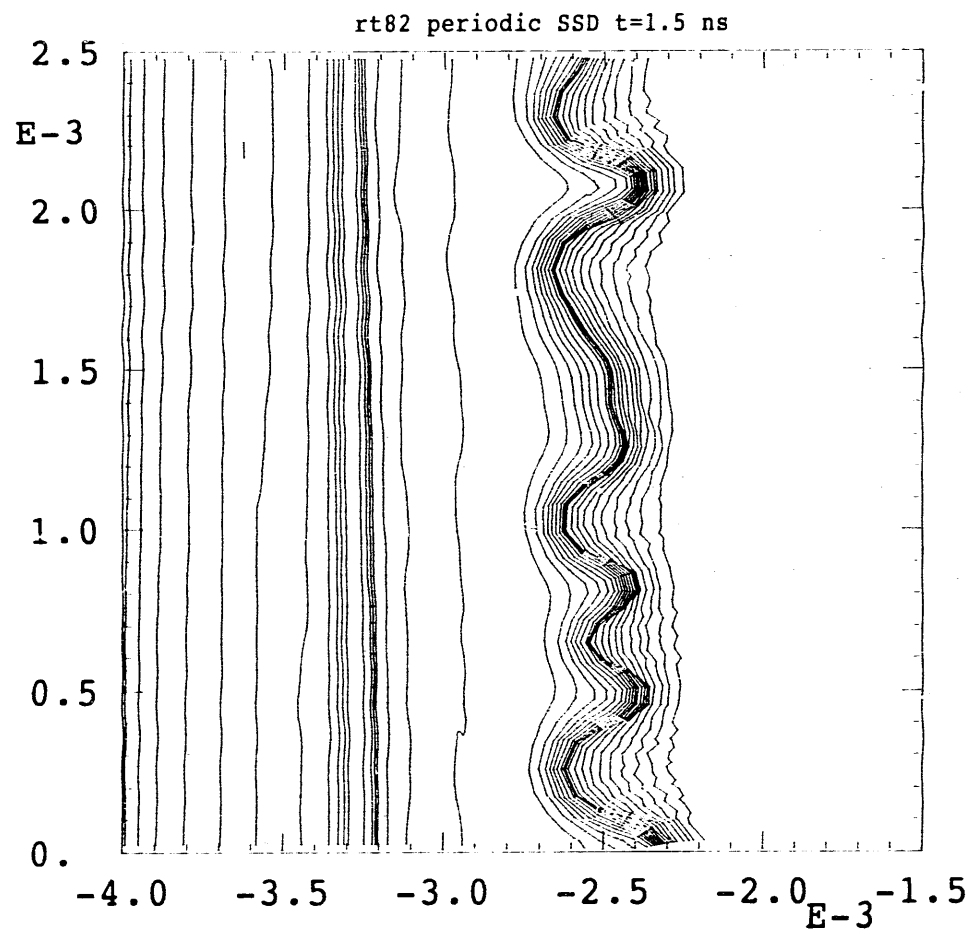

density contours

time = 1.5 ns

Figure 13b.

Reference UCRL-JC-104372

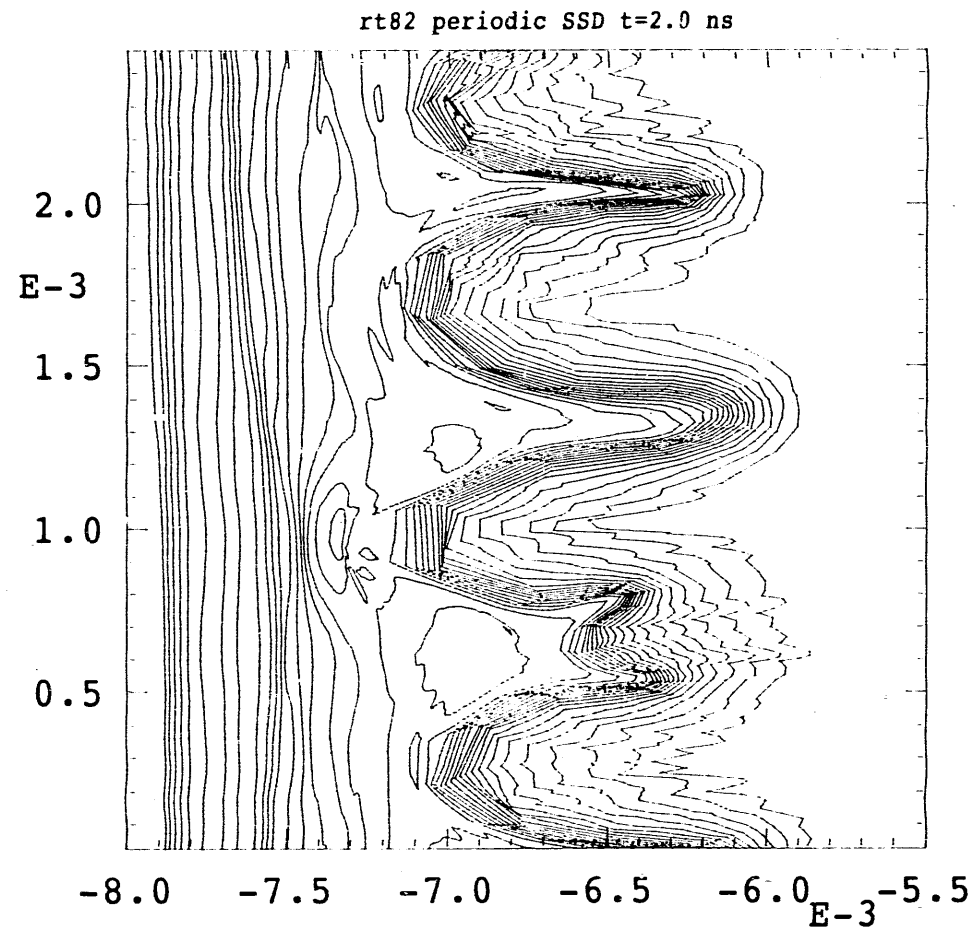

density contours

time = 2.0 ns

Figure 13c.

Reference UCRL-JC-104372

calculations predict more rapid ablation with nonuniform illumination

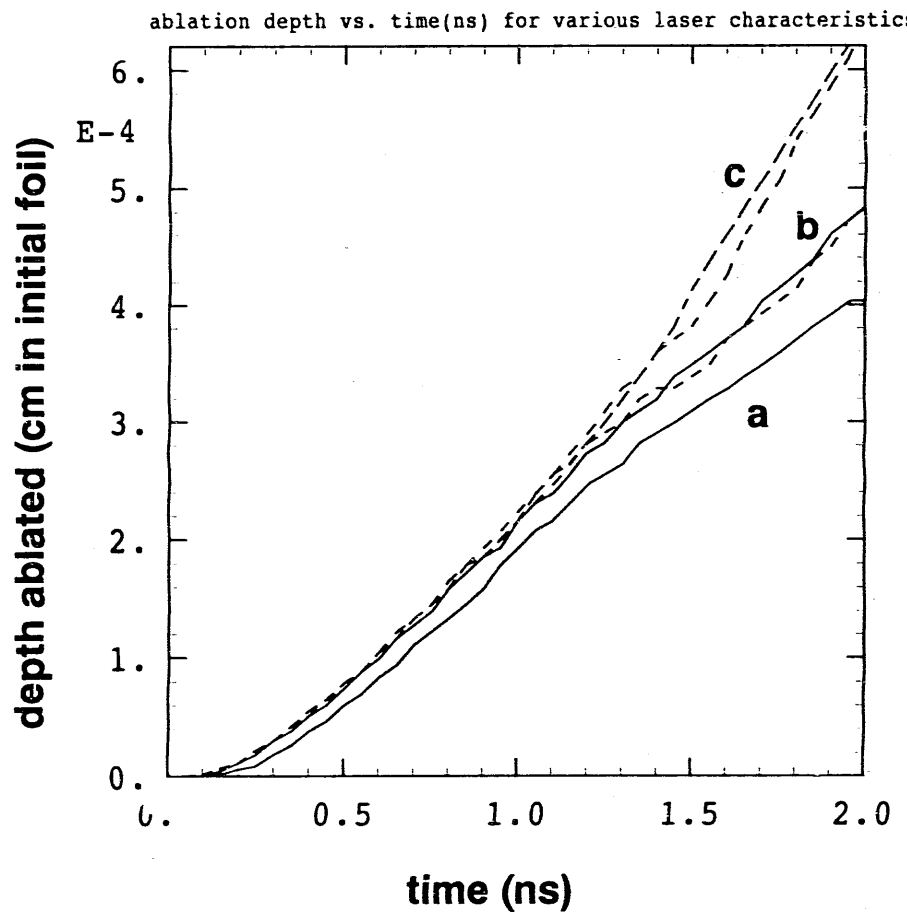

a - 1-D calculation

b - average depth in calculations with RPP (solid), SSD (dash)

c - maximum depth in calculations with RPP (longer dash), SSD

Figure 14.

Reference UCRL-JC-104372

rise time of emission lines from seeded layer indicates enhanced ablation rate

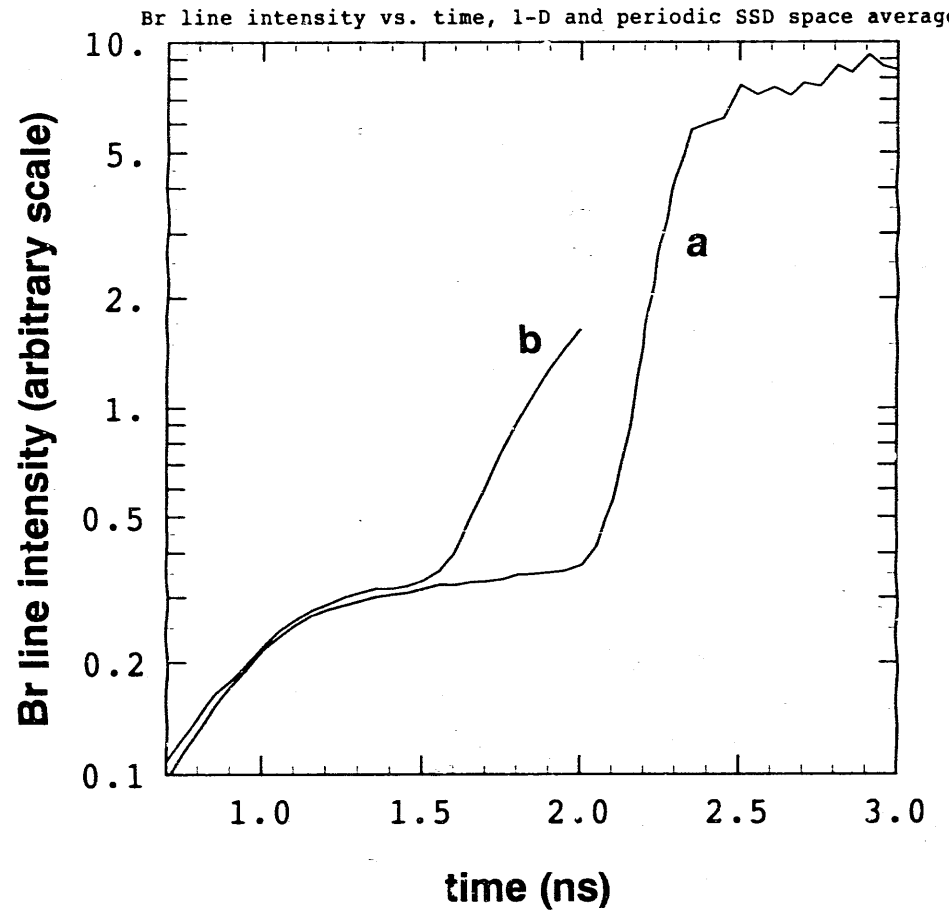

a - 1-D calculation, 3% Br layer under 4 μm CH

b - RPP calculation, spatial average

Figure 15.

Reference UCRL-JC-104372

END

DATE FILMED

12 / 31 / 90